Study of Noise Generation Using the Eppler 387, NACA 0012, NACA 4412 and NREL S823 Airfoils

Andrew Hays
Master of Science in Mechanical Engineering Candidate
Baylor University

Kenneth W. Van Treuren
Graduate Advisor
Department of Mechanical Engineering
Baylor University

Abstract

Renewable energy is needed now more than ever to meet current demands as conventional energy sources are being depleted. Wind energy has the potential to provide a substantial amount of energy but more research must be done. Of increasing interest is the development of small wind turbines for residential and urban applications. This research focuses on the airfoils used on small scale, fixed-pitch horizontal-axis wind turbines and the noise that the airfoils produce. Noise measurements were taken for the Eppler 387, NACA 0012, NACA 4412 and NREL S823 Airfoils. These airfoils were tested at Reynolds numbers ranging from 50,000 to 200,000, with angles of attack ranging from -10 to 25 degrees, and with a chord length of 6 in. The noise was measured at frequencies ranging from 12.5 Hz to 20,000 Hz for each data point. The A-Weighted value was recorded. Understanding noise generation on airfoils will help in the design of quieter wind turbines for more populated areas.

Introduction

The energy demands of the modern world have reached an all-time high and the current amount of energy produced with fossil fuels will not keep pace with the demands. Due to the continuous use of fossil fuels across the world and the instability of the Middle East region, the shortage of these resources can become a reality at almost any time. The need for renewable energy is extremely important and powering the world with renewable energy sources is a desired solution to create a sustainable future. The different sources of renewable energy include: solar power, wind power, geothermal, and hydroelectric. Within the topic of wind power, there are two major categories; large-scale wind farms, and single, smaller wind turbines. Wind farms contain multiple turbines capable of producing megawatts of power. In contrast, single, smaller wind turbines have been categorized with different definitions, but the most consistent being the following: micro-wind, up to 1 kW, small wind, from 1-50 kW and medium wind, ranging from 50 kW up to 500 kW [1][2].

The advantage of smaller wind turbines is that producing power near where it will be used, can save millions of dollars in transmission lines [3] and can help lower the footprint of power line structures across the country. Within small wind research is being done to design airfoils to maximize power

production when coupled with the most efficient generators. Another important topic is aero acoustic research, studying the noise produced by these small turbines. These small turbines rotate on the order of several hundred to several thousand RPM, depending on their size, compared to large turbines that rotate at a rate of 15-50 RPM [4]. These high rotational speeds of small wind turbines create high levels of noise. Small turbines located in suburban or urban areas create a need to lower the acoustic footprint.

Wind turbine noise can be broken into 6 categories [5-7]:

1. Trailing Edge Noise: Noise due to boundary layer development which transitions to turbulence and the interaction between the turbulent eddies and the trailing edge creates a major source of noise [8][9]

2. Separation-Stall Noise: Noise due to a high angle of attack of the wind turbine blade creating large separation wake.

3. Laminar Boundary Layer Vortex Shedding: Noise that is created when a laminar boundary layer is present over the blade resulting in a feedback loop excited pressure waves. This noise is amplified in the boundary layer.

4. Tip Vortex Formation: Noise that is created due to the vortices generated by flow at the tips of the turbine blade.

5. Trailing Edge Bluntness Vortex Shedding: Noise generated at the blunt trailing edges of the turbine blade. This source is controlled by the shape of the trailing edge of the airfoil blade.

6. Turbulent Inflow Noise: Noise that is generated based on the incoming turbulence of the free stream air contacting the airfoil's leading edge.

This study will investigate the trailing edge noise and the separation-stall noise of the Eppler 387, NACA 0012, NACA 4412 and NREL S823 Airfoils. When recording noise values, the range of frequencies measured is from 12.5 to 20,000 Hz. The human ear is not sensitive to the individual frequencies except for at the extremes. There are frequency "weighting" systems that are known as A-Weighted and C-Weighted. The A-Weighted system is a filtration system that conforms to the hearing levels of the human ear. The C-Weighted system is a similar filtration system but is focused on highlighting very loud or very low frequency sounds [10]. For the purpose of this research, the A-Weighted system will be used to compare the generated sound.

Testing Apparatus

All wind tunnel tests were performed in the Baylor Subsonic Wind Tunnel, seen in figure 1. It is an Engineering Laboratory Design, Inc. (ELD) Model 406B. This wind tunnel is open-circuit and has a constant-pitch fan driven by a variable-speed, 40-hp motor, which allows wind speeds in the tunnel to range from 0.1-50 m/s. The test section is 4 ft. long with a 2 ft. square cross section. The tunnel velocity variation is ±1% and the turbulence intensity is less than 0.2% at the inlet to the test section. A Brüel & Kjaer (B&K) G-4 2270 Handheld Frequency Analyzer was connected to a ¼" microphone, both can be seen in figure 2. To begin the process, the microphones were calibrated using the Brüel & Kjaer Type 4231 calibration system to ensure accurate results. The B&K microphone was set in the wind tunnel on

the vertical center of the wind tunnel, 2.5 chord lengths (15 inches) downstream of the airfoils. This setup of the wind tunnel can be seen in figure 1. Two of the airfoils tested were constructed from foam and finished with an epoxy resin; these were the National Renewable Energy Laboratory (NREL) S823 and Eppler 387 2D airfoils. The Eppler 387 which can be seen in figure 3 [11]. The NACA 0012 and NACA 4412 were commercial models made by ELD and were constructed of resin. The NACA 0012 can be seen in figure 4. An ELD force balance was used as a stand to hold the airfoils in place. The airfoils were tested at angles of attack (AOA) ranging from -10 to 25 degrees. The AOA for each test was measured with a Craftsman 7-inch Digital Torpedo Level. A LabVIEW VI was constructed to operate the wind tunnel and monitor the atmospheric conditions. The wind tunnel was controlled by using an NI-cDAQ 9178 chassis containing an NI 9263 AO channel to control the tunnel and an Omega zSeries zED-THPB-LCD was used to read the atmospheric conditions to the VI for Reynolds number calculations. The airfoils were set at a distance of 9 inches from the entrance of the tunnel. The testing was done at Reynolds numbers of 50,000, 75,000, 100,000, 125,000, 150,000 and 200,000. These numbers were calculated using the wind speed of the tunnel, measured by a PCL-2A differential pressure transducer, the chord length of 6 inches, and fluid properties of the air.

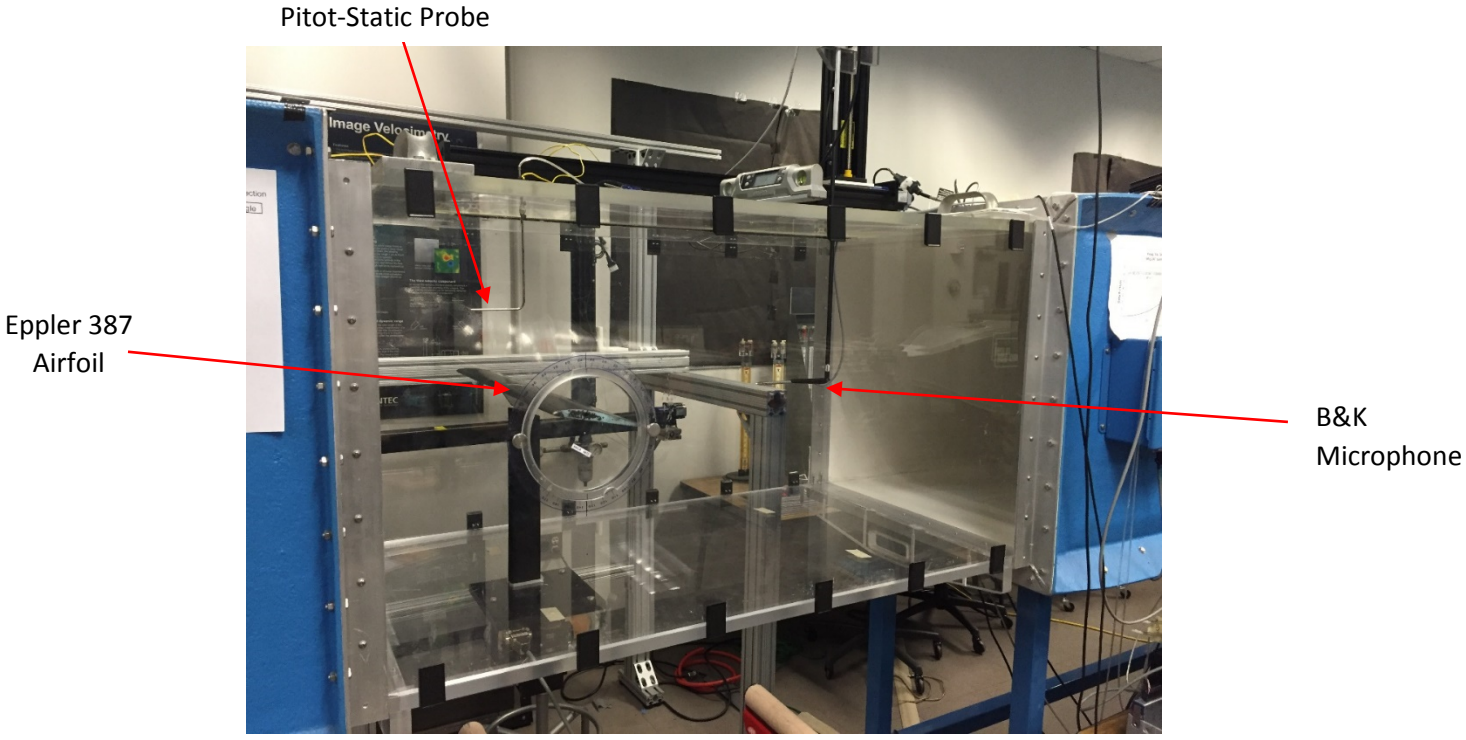

Figure 1. Experimental Wind Tunnel Setup

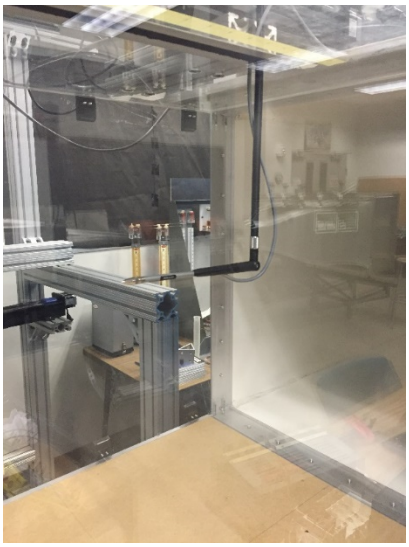

Figure 2. Brüel & Kjaer ¼" Microphone and G-4 2270 Frequency Analyzer

Figure 3. Eppler 387 on Test Stand

Figure 4. NACA 0012 on Test Stand

Airfoils Tested

The airfoils that were tested in this experiment were chosen based on their availability in the lab as well as their current or former use on wind turbines. The Eppler 387 in figure 5 is an airfoil that is used on wind turbines today, but typically on a larger scale. These blades are operated at relatively low Reynolds Numbers of 60,000 to 500,000 [12]. The NACA 0012 in figure 6 was chosen to study to see the effects of symmetry on noise generation. The NACA 0012 was also an airfoil that was used on early wind turbines due to extensive knowledge of its performance characteristics. The NACA 4412 in figure 7 was chosen due to its early use on wind turbines, similar to the NACA 0012. The 4412 and the 4415 were two of the airfoils chosen for early wind turbine design due to extensive knowledge of their performance. The NREL S823 in figure 8 was developed for small sized, stall-regulated, horizontal-axis wind turbines, defined by NREL as 3 to 10 meters in diameter [13]. The large leading edge was designed for lower wind speeds to keep the flow attached for lower Reynolds Numbers.

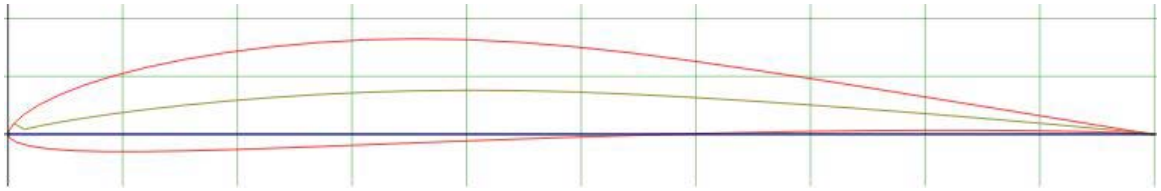

Figure 5. Eppler 387 Airfoil [14]

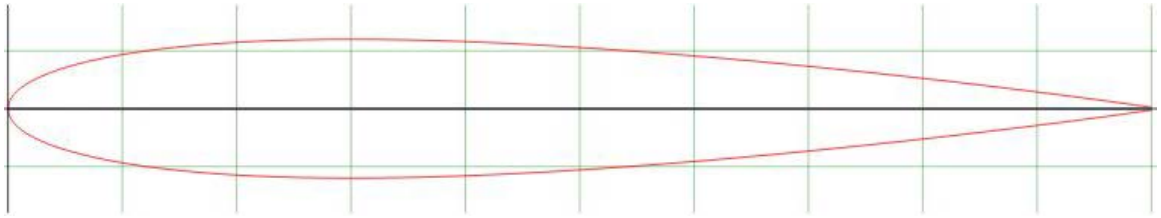

Figure 6. NACA 0012 Airfoil [14]

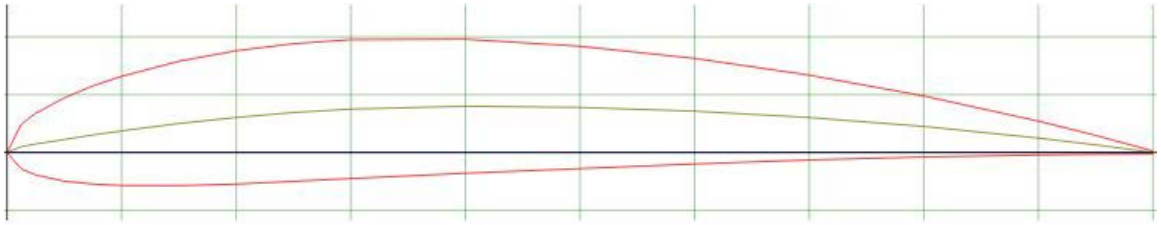

Figure 7. NACA 4412 Airfoil [14]

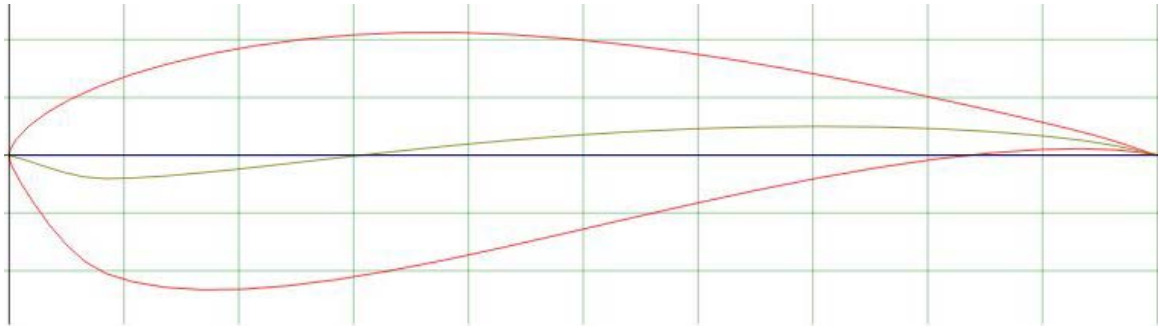

Figure 8. NREL S823 Airfoil [14]

Uncertainty Analysis

For this experiment, the values of uncertainty reported came from the manufacturers uncertainty for the device used. The Craftsmen Digital Torpedo Level has a rated uncertainty of ±0.1°. The B&K microphone and analyzer have a rated uncertainty of ±1.5 dB. The Reynolds number calculations were made based on the values of velocity, given from the PCL-2A differential pressure transducer connected to a pitot-static probe in the tunnel and the atmospheric properties given from the Omega zSeries zED-THPB-LCD. The PCL-2A differential pressure transducer has a rated uncertainty of ±0.07% span. The Omega atmospheric conditions monitor has a rated uncertainty of ±0.5°C and ±2 mbar.

Experimental Procedure

The microphone was set at the desired location in a clean tunnel (except for an upstream pitot-static probe). The wind tunnel was then run at a series of settings to determine the voltages corresponding to the Reynolds numbers of interest. Once the desired Reynolds numbers were set, the microphone collected data at one minute testing intervals to assess the background noise in the clean tunnel used later during data reduction. After completing these tests, the airfoil was put into the wind tunnel and mounted on the force balance. With this setup, the airfoil was then placed at an AOA of -10 degrees, measured by the Craftsmen level. The testing then commenced at each Reynolds number with the microphones collecting data for one minute intervals at each set value. After each set of measurements, the airfoil was changed to the next AOA, and the testing was done again. The AOA's studied were -10, -5, 0, 5, 10, 11, 12, 13, 14, 15, 17, 20 and 25. The AOA of 10-17 were studied in one degree increments because these values are near the airfoil stall AOA where the separation increases which greatly increases the noise downstream of the airfoil. After testing one airfoil, the next airfoil was put in the tunnel and tested until all four airfoils had been completed. Once this process was completed, the A-Weighted values collected from the Brüel & Kjaer handheld analyzer were corrected for background noise using equation 1 [10]

$$\boldsymbol{Noise_{Corrected} = 10 * \left(Log_{10} \left(10^{\left(\frac{NoiseLevel}{10}\right)} - 10^{\frac{CleanNoise}{10}} \right) \right)} \quad \textbf{(1)}$$

From corrected noise values, the Reynolds Numbers, and the measured Angles of Attack, the following graphs were examined for trends.

Results

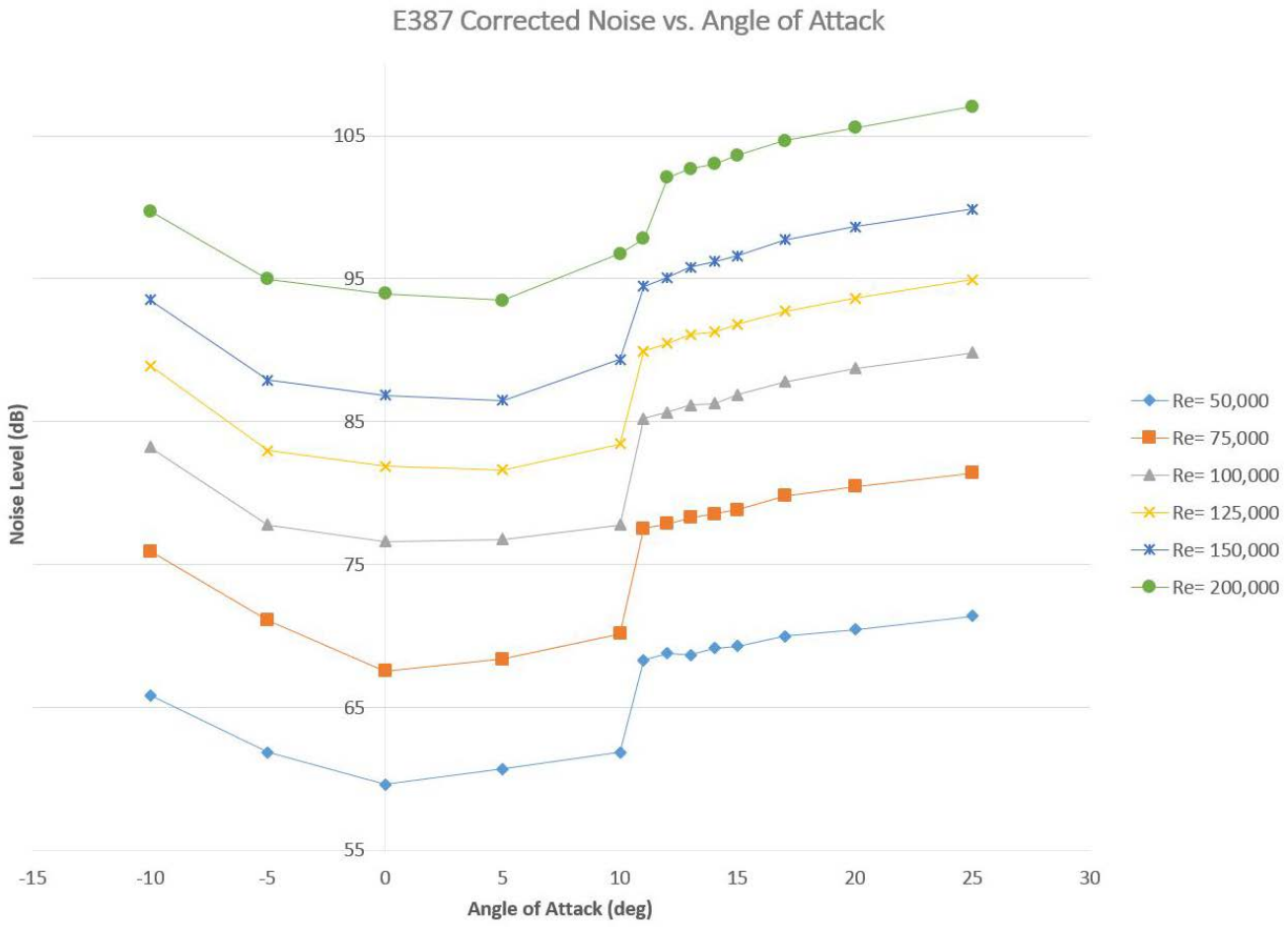

Figure 9. Eppler 387 Noise Level vs. Angle of Attack

The Eppler 387 shows that as the Reynolds number increases in 25,000 increments, the sound pressure level (SPL) increases at a consistent 10 dB interval up until 100,000 after which the increase is reduced by approximately half. This change is thought to be due to the higher Reynolds numbers having more energy and causing less separation. As the AOA changes from -10 to 5, the noise level decreases due to the flow having less separation as the angle approaches 5 degrees. The stall point of the airfoil can be seen to occur at the increase in SPL around an AOA of 10 degrees. The stall condition creates a large amount of separated flow, which creates a step increase in noise. After stall induced separation, the SPL continues to rise, but at a much lower rate compared to the initial increase from stall. At a Reynolds Number of 200,000 the stall is delayed until 11 degrees. This delay in stall is due to the greater amount of energy in the flow, thus, keeping the SPL lower until full stall at 11-12 degrees. The highest SPL measured for this airfoil was 107 A-Weighted decibels (dB(A)) at a Reynolds Number of 200,000 and an AOA of 25 degrees.

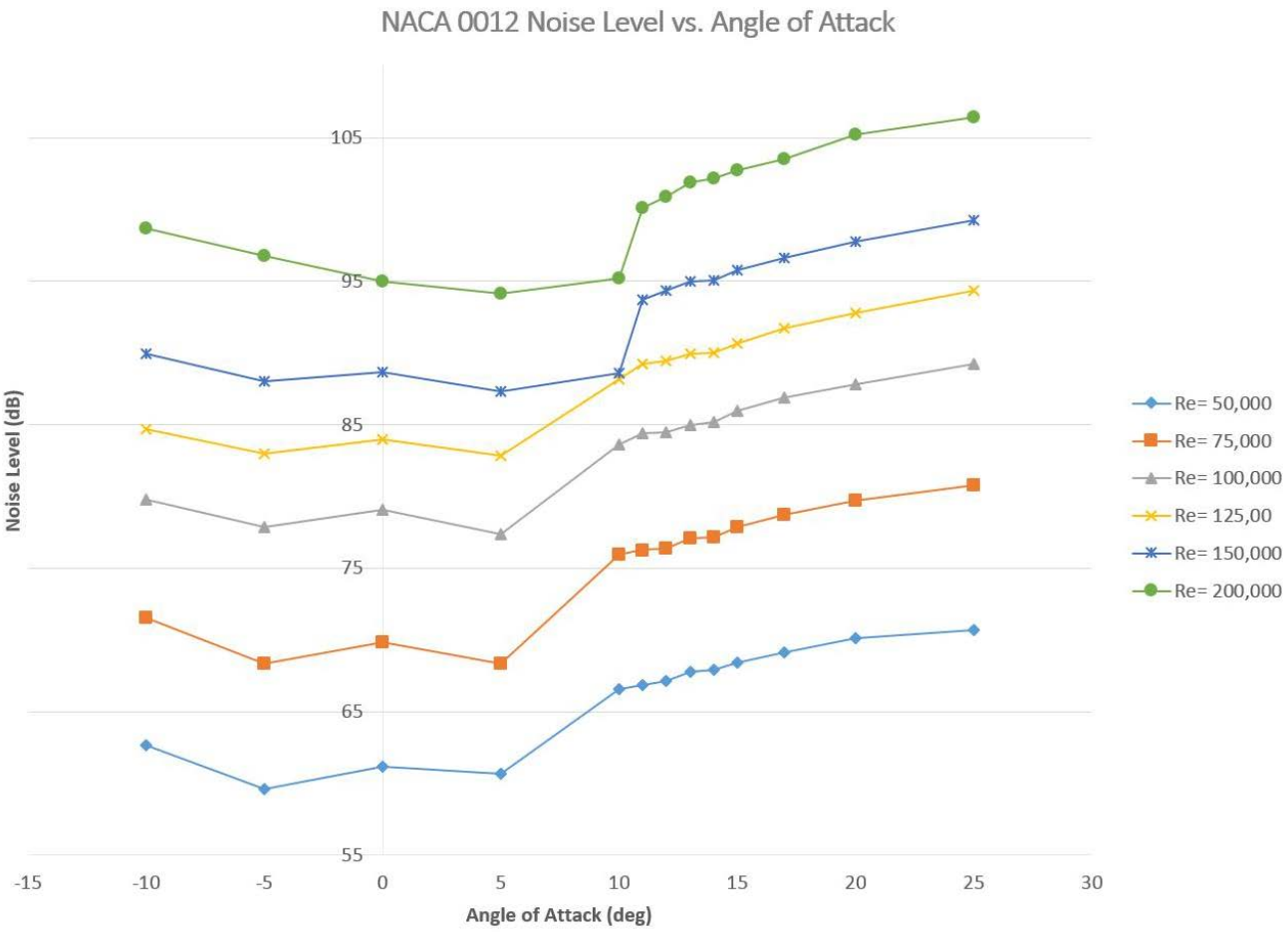

Figure 10. NACA 0012 Noise Level vs. Angle of Attack

The NACA 0012 showed similar trends to the E387 in that as Reynolds Number and AOA increased, the SPL did as well. Since the NACA 0012 is a symmetric airfoil, it did show interesting characteristics at the negative angles and their positive counterparts. For -5 and 5 degrees AOA, the SPL values were very close, as expected due to the symmytry of the airfoil, although for -10 and 10 degrees AOA this was not the case. Timmer [15] studied a 2D NACA 0018 airfoil, and found that the symmytric profile of the airfoil does not always act as intended at lower Reynolds Numbers, around 150,000 and below. This helps explain why the data is not entirely consistent for the corresponding positive and negative angles. Strong separation occurs on this airfoil somewhere between 5 and 10 degrees for the Reynolds Numbers 50,000 to 125,000. For the two higher Reynolds Numbers, the increased energy keeps the flow attatched at higher angles of attack, stalling around 10 degrees AOA. The highest SPL measured for this airfoil was 106.5 db(A) at a Reynolds Number of 200,000 and an AOA of 25 degrees.

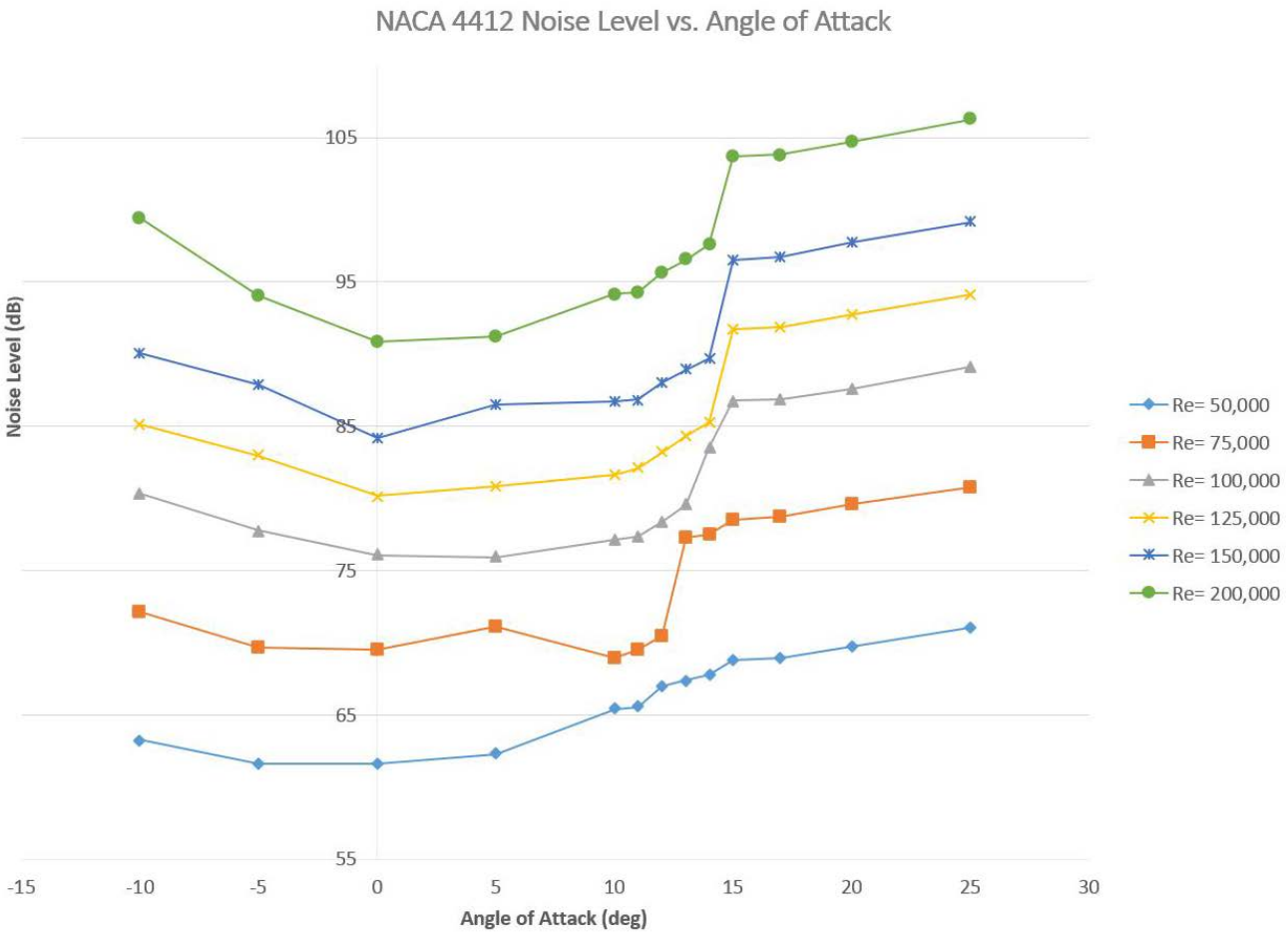

Figure 11. NACA 4412 Noise Level vs. Angle of Attack

The NACA 4412 continued to show similar trends as the previous two airfoils, however this airfoil exhibited new trends. For a Reynolds Number of 50,000, the SPL was relatively constant from -10 degrees up until 5 degrees, only changing by 1.5 dB(A). The increase from 5 to 10 degrees is less drastic then the other separation increases seen at the higher Reynolds Numbers. At a Reynolds Number of 75,000, the SPL stays relatively constant, similar to Reynolds number of 50,000, but the separation increase is distinctive, similar to the higher Reynolds numbers. After the drop of 2 dB(A) from 5 to 10 degrees AOA, the SPL rises until the stall separation increase at an AOA of 13 degrees, and then continues to follow the expected trends that have been seen thus far. The four higher Reynolds numbers follow the expected trends that have been recognized in the previous tests. The only difference between these four tests is the separation point for the Reynolds number of 100,000, which begins stall separation at 13 degrees while the other three do not see stall separation until 14 degrees. The highest SPL measured for this airfoil was 106.25 dB(A) at a Reynolds Number of 200,000 and an AOA of 25 degrees.

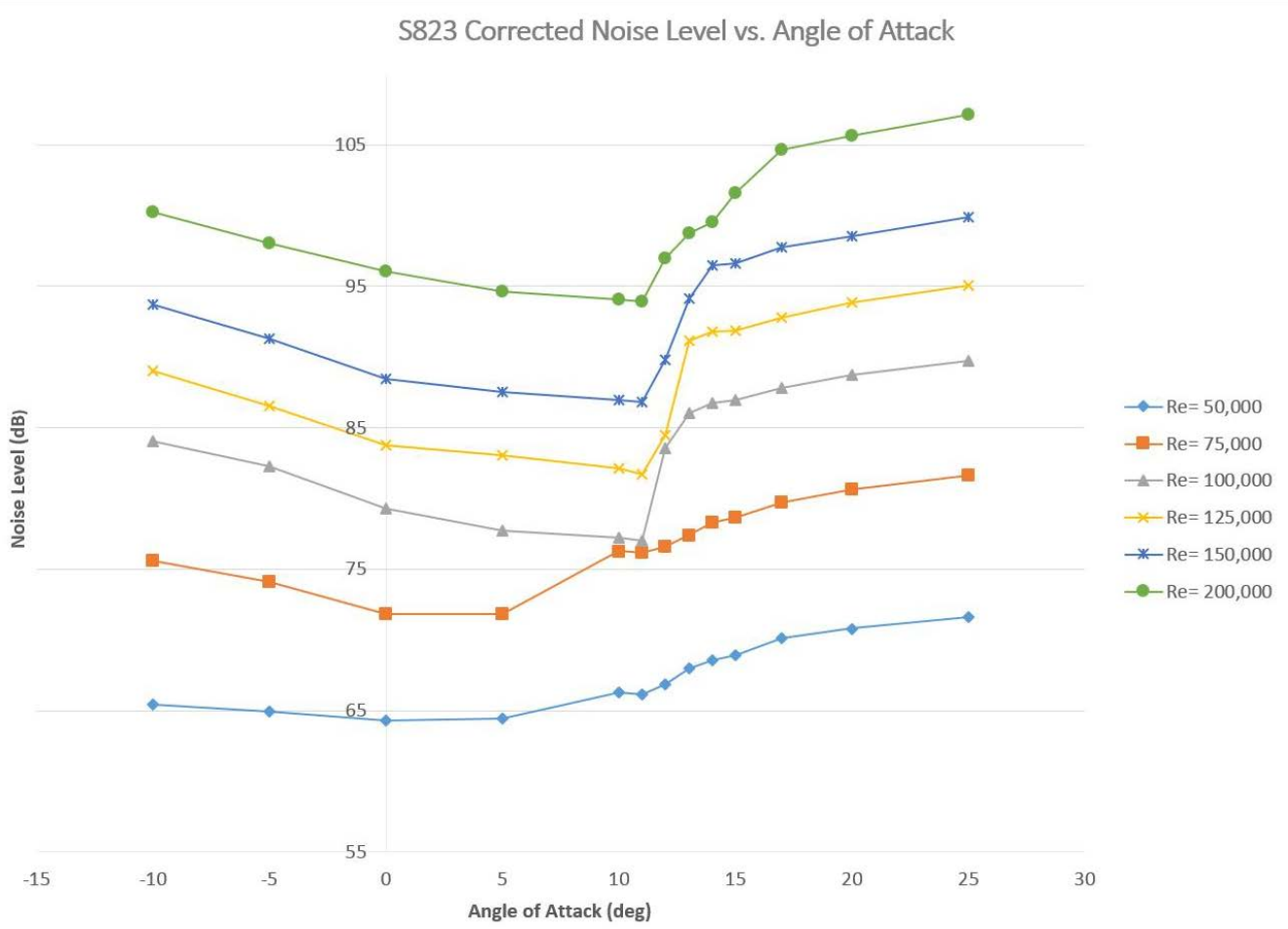

Figure 12. NREL S823 Noise Level vs. Angle of Attack

For the NREL S823, the trends observed regarding increasing Reynolds number were similar, but AOA trends were not consistent with previous trends. Due to the large leading edge of the S823, the negative and low angles of attack all have a constant or decreasing SPL due to the flow reattaching to the bottom of the airfoil. For the 50,000 Re case, the SPL slowly increases up to its maximum with a relatively small stall separation increase of 2 dB(A) at 10 degrees. At a Reynolds number of 75,000, the same trend is followed, except the separation increase is greater with a value of 6 dB(A). For the next three Reynolds numbers, they follow the same trends as the previous airfoils in regards to the stall separation increase at 11 degrees, and then a relatively flat slope beyond the increase. At 200,000, the flow separation is delayed and there are small jumps between 11-15 degrees and then SPL follows the same trends as the lower Reynolds numbers. The highest SPL measured for this airfoil was 107 dB(A) at a Reynolds number of 200,000 and an AOA of 25 degrees.

Flow Separation

As flow interacts with the airfoil, the flow either stagnates at the leading edge or flows over the top and bottom surfaces of the airfoil. The flow begins to separate after a short distance across the chord of the blade, but this separation is minimal at low AOA and does not affect the lift characteristics of the airfoil. As AOA increases separation increases, working its way from the trailing edge of the airfoil to the leading edge. Stall occurs when the AOA increases to a point where the flow can no longer stay attached to the airfoil. Stall separation causes the lift force to dramatically drop when the flow is no longer attached on the top surface of the airfoil. This large separation is what creates high levels of noise coming off of the trailing edge of each airfoil. The stall point is critical to know due to the noise generation increase at stall. As seen in figures 9-12, once stall is reached, the SPL increases greatly, around 10-15 degrees AOA. In figure 13, lift and drag data at a Reynolds number of 100,000 is shown for the NREL S823 airfoil.

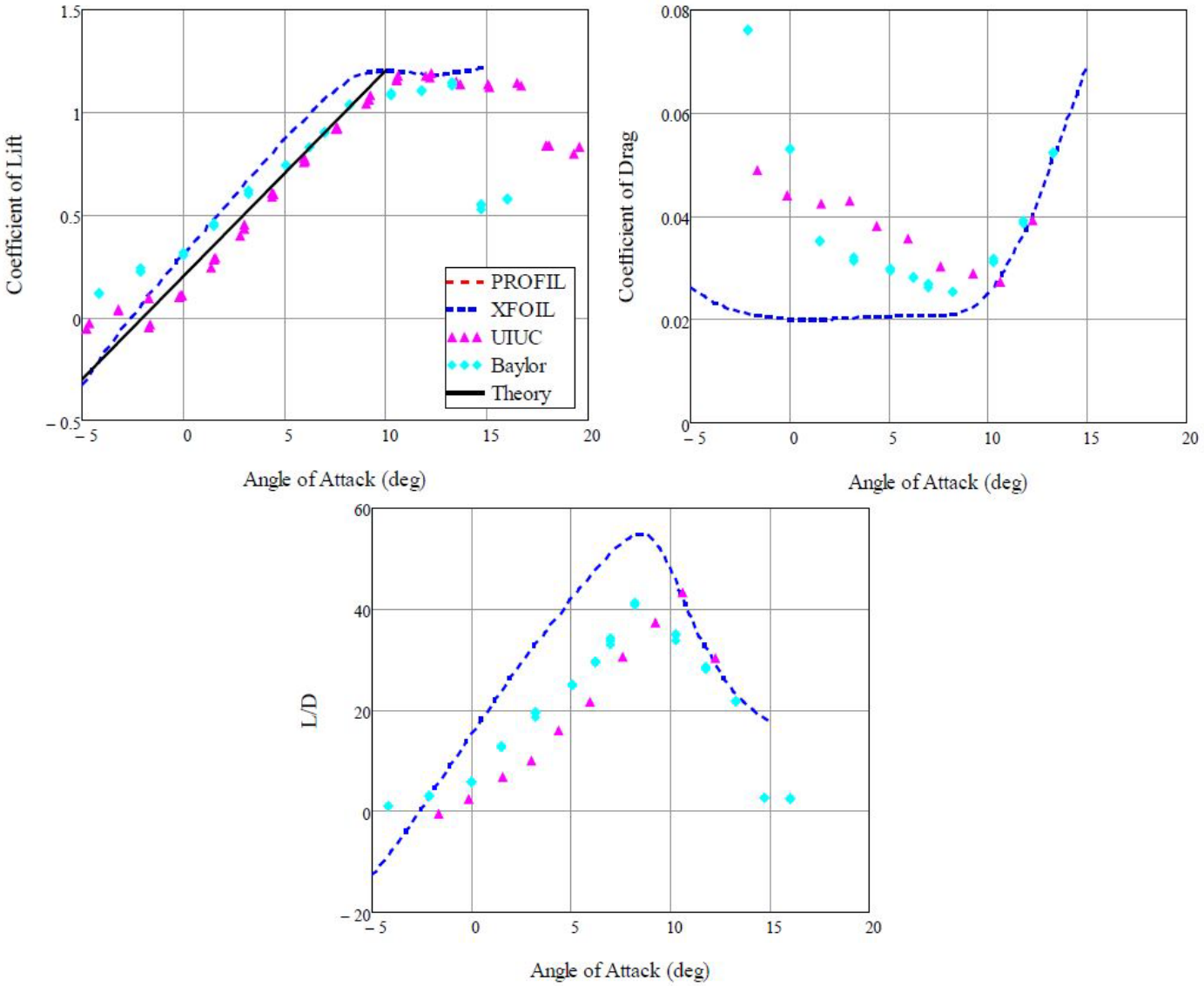

Figure 13. NREL S823 Airfoil Data at Re=100,000 [11][16]

With this data, it shows that the stall AOA for the S823 occurs at roughly 12 degrees, while the noise data shows stall separation SPL increase to occur from 11-12 degrees. This agreement shows that the stall separation of the flow on the airfoil does indeed cause the sharp increase of noise generated off of the airfoil. The L/D graph shows that the highest efficiency occurs at an AOA of approximately 9 degrees. The noise data shows that at 9 degrees AOA, operating at a Reynolds number of 100,000, the airfoil is generating very near the lowest noise level possible for that Reynolds number. In table 1, the CL-Max, AOA-Stall, and L/D max for each airfoil is listed for a Reynolds number of 100,000. This data shows that the other 3 airfoils follow the same trends in regards to stall separation and the increase in noise generation at the stall AOA. The CL-max and L/D max show the design points for the airfoils and where their power production can be maximized. This design point now has a corresponding SPL that the airfoil will emit when subject to a Reynolds number of 100,000. With these two sets of data, the power production of the airfoil can be estimated along with the noise generation.

Table 1. Airfoil Data at Re=100,000 [14]

Airfoil	CL-Max	AOA-Stall	L/D Max
Eppler 387	1.30	12°	60.7 at 7.5°
NACA 0012	1.00	10.5°	36.7 at 5°
NACA 4412	1.48	13°	56.1 at 8.5°
NREL S823	1.25	12°	42.3 at 9.25°

Conclusions & Future Work

The main trend is that the noise levels increase at a steady rate based on angle of attack and Reynolds number. These tests show that the airfoils can create a substantial amount of noise and it must be a consideration when designing a wind turbine. These results show that for each airfoil, there are advantages and disadvantages to each one regarding noise generation depending on the flow conditions that are expected. Based on the noise data from this study, the NACA 4412 should be chosen for its low SPL values at the medium angles of attack, 0-10 degrees. The 4412 consistently showed lower SPL values and the stall separation begins to occur at 11 degrees AOA. The 4412 showed that stall separation occurred around 13-15 degrees AOA, depending on the Reynolds number. This higher stall AOA gives the 4412 an advantage such that it has a greater range of angles before it stalls and stops producing power and generates more noise.

Future work can be done with this data as a basis for noise optimization. The first step of optimization can done by adjusting the airfoil shape. This can be done by changing the size of the leading and trailing edges, the camber of the airfoil, or placing trip strips on the airfoil. A high stall AOA with a high CL value is desired. For a wind turbine, the optimum angle for design is usually at L/D max, so this value should be as high as possible. Besides airfoil optimization, airfoils that are currently used on small wind turbines can be tested for their noise generation and compared with the airfoils from the current tests. Once testing of the airfoils is completed, the optimization process for the blades can begin. With each blade iteration, lift and drag force must be measured either experimentally or using a CFD program such as XFOIL, to show that the blade still has good lift and drag characteristics. These tests of the new blades can be compared to their original counterparts, and then an optimum blade can be fabricated for small wind turbines depending on the conditions that are expected.

References

[1] Renewable UK. Small and Medium Wind UK Market Report. October 2013.

[2] Clausen, P. D., and Wood, D. H., 1999, "Research and Development Issues for Small Wind Turbines," Renewable Energy, 16, pp. 922-927.

[3] Alonso, F., and Greenwell, C. A. E., 2013, "Underground vs. Overhead: Power Line Installation-Cost Comparison and Mitigation" from: http://www.elp.com/articles/powergrid_international/print/volume-18/issue-2/features/underground-vs-overhead-power-line-installation-cost-comparison-.html

[4] Chiras, D., Sagrillo, M., and Woofenden, I., 2009, *Power from the Wind*, New Society Publishers, Canada.

[5] Ning, S., Damiani, R., and Moriarity, P., 2013, "Objectives and Constraints in Wind Turbine Optimization," AIAA 2013-0201, 51st AIAA Aerospace Sciences Meeting, January 7-10, 2013, Grapevine, TX.

[6] PROPID, http://m-selig.ae.illinois.edu/propid.html accessed on November 24, 2015.

[7] Wright, A. K., and Wood, D. H., 2004, "The Starting and Low Wind Speed Behavior of a Small Horizontal Axis Wind Turbine," Journal of Wind Engineering and Industrial Aerodynamics", 92, pp 1265-1279.

[8] XFOIL, http://web.mit.edu/drela/Public/web/xfoil/ accessed on November 24, 2015.

[9] XFLR5, http://www.xflr5.com/xflr5.htm accessed on November 24, 2015.

[10] "Environmental Noise", 2000, Brüel &Kjaer Sound & Vibration Measurement A/S

[11] Burdett, T., 2012, "Aerodynamic Design Considerations for Small-Scale, Fixed-Pitch, Horizontal-Axis Wind Turbines Operating in Class 2 Winds," M.S. Thesis, Mechanical Engineering, Baylor University

[12] Amano, R. S., and Sunden, B., 2015, *Aerodynamics of Wind Turbines: Emerging Topics,* WIT Press, Billerica, MA., Chap. 4.

[13] http://www.nrel.gov/docs/fy05osti/36342.pdf

[14] Airfoil Tools, 2015, airfoiltools.com, generated using XFoil

[15] Timmer, W. A., 2008, "Two-dimensional low-Reynolds number wind tunnel results for airfoil NACA 0018", Wind Engineering, 32(6), pp. 525-537.

[16] Selig, M. S., Guglielmo, J. J., Broeren, A. P., and Giguère, P., 1995, Summary of Low-Speed Airfoil Data, Vol. 1, SoarTech Publications, Virginia Beach, VA.